

## Electronic Supplementary material

for manuscript

### Metallophilic interactions in Ag-dicyanoaurate compounds

Emanuele Priola<sup>a,\*</sup>, Alessia Giordana<sup>a</sup>, Rosa M. Gomila<sup>b</sup>, Ennio Zangrando<sup>c</sup>, Luca Andreo<sup>a</sup>, Roberto Rabezzana<sup>a</sup>, Lorenza Operti<sup>a</sup>, Eliano Diana<sup>a</sup>, Ghodrat Mahmoudi<sup>d,e,\*</sup> and Antonio Frontera<sup>\*,b</sup>

---

<sup>a</sup> Department of Chemistry, University of Turin, via P. Giuria 7, 10125 Torino, Italy. E-mail: emanuele.priola@unito.it

<sup>b</sup> Departament de Química, Universitat de les Illes Balears, Crta de Valldemossa km 7.5, 07122 Palma de Mallorca (Balears), SPAIN. E-mail: [toni.frontera@uib.es](mailto:toni.frontera@uib.es)

<sup>c</sup> Department of Chemical and Pharmaceutical Sciences, University of Trieste, Via L. Giorgieri 1, 34127 Trieste, Italy

<sup>d</sup> Department of Chemistry, Faculty of Science, University of Maragheh, P.O. Box 55181-83111, Maragheh, Iran. E-mail: ghodratmahmoudi@gmail.com

<sup>e</sup> «Advanced Materials for Industry and Biomedicine» laboratory, Kurgan State University, Sovetskaya Str. 63/4, 640020 Kurgan, Russian Federation

#### Table of contents:

1. Tables S1 to S5	Page 2
2. ESI mass spectrometry	Page 5

**Table S1.** Crystallographic Data and Details of Refinements for complexes **1-4**

	<b>1</b>	<b>2</b>	<b>3</b>	<b>4</b>
empirical formula	C <sub>30</sub> H <sub>18</sub> Ag <sub>2</sub> Au <sub>2</sub> N <sub>10</sub>	C <sub>30</sub> H <sub>18</sub> Ag <sub>2</sub> Au <sub>2</sub> N <sub>10</sub>	C <sub>17</sub> H <sub>11</sub> AgAuN <sub>5</sub>	C <sub>43</sub> H <sub>27</sub> Ag <sub>4</sub> Au <sub>4</sub> N <sub>15</sub>
fw	1128.22	1128.22		1973.14
cryst system	triclinic	monoclinic	monoclinic	triclinic
space group	<i>P</i> $\bar{1}$	<i>P</i> 2 <sub>1</sub> / <i>c</i>	<i>P</i> 2 <sub>1</sub> / <i>n</i>	<i>P</i> $\bar{1}$
<i>a</i> (Å)	7.2797(13)	12.0660(7)	6.8295(5)	11.3724(8)
<i>b</i> (Å)	9.847(4)	16.5009(8)	16.5330(10)	14.8294(10)
<i>c</i> (Å)	10.868(3)	7.4390(5)	14.7584(8)	16.3394(11)
$\alpha$ (°)	86.98(3)	90	90	116.322(7)
$\beta$ (°)	79.08(2)	100.028(6)	101.314(6)	95.174(5)
$\gamma$ (°)	83.75(2)	90	90	101.927(6)
<i>V</i> (Å <sup>3</sup> )	760.0(4)	1458.48(15)	1634.02(18)	2364.0(3)
<i>Z</i>	1	2	4	2
<i>D</i> <sub>calcd</sub> (mg/m <sup>3</sup> )	2.465	2.569	2.399	2.772
$\mu$ (Mo-K $\alpha$ ) (mm <sup>-1</sup> )	10.930	11.392	10.174	14.031
<i>F</i> (000)	520	1040		1788
$\theta$ range (°)	3.37 - 26.37	3.25 - 30.51		3.22 - 26.37
collected reflections	6139	37750	28212	21036
indep reflections	3091	4451	3343	9662
<i>R</i> <sub>int</sub>	0.1583	0.0945	0.0737	0.0483
Obsd refls <i>I</i> > 2 $\sigma$ ( <i>I</i> )	1069	3111	2264	5331
parameters	199	199	220	595
GOF on <i>F</i> <sup>2</sup>	0.934	1.023	0.983	1.071
<i>R</i> 1 [ <i>I</i> > 2 $\sigma$ ( <i>I</i> )] <sup>a</sup>	0.0972	0.0453	0.0304	0.0644
<i>wR</i> 2 [ <i>I</i> > 2 $\sigma$ ( <i>I</i> )] <sup>a</sup>	0.1507	0.0788	0.0649	0.1041
residuals (e Å <sup>-3</sup> )	1.359, -1.830	1.387, -0.814	0.695, -0.421	1.752, -0.887

<sup>a</sup>  $R1 = \sum ||F_o| - |F_c|| / \sum |F_o|$ ,  $wR2 = \sum w (F_o^2 - F_c^2)^2 / \sum w (F_o^2)^2 ]^{1/2}$

**Table S2.**  $\pi\cdots\pi$  ring interaction and  $\pi\dots$ Metal distances (Å) and angles ( $^{\circ}$ ) for compound **1**<sup>a</sup>

$\pi\cdots\pi$ ring interaction							
Cg(I)	Cg(J)	Symmetry Cg(j)	Cg(I)-Cg(J)	$\alpha$	$\beta$	$\gamma$	slippage
pyN3	pyN4	-x, 1-y, 1-z	3.764(17)	1.	22.6	21.4	1.447
pyN4	pyN3	-x, 1-y, 1-z	3.764(17)	1.	21.4	22.6	1.374
$\pi\dots$ gold interaction							
pyN4	Au		3.998		29.51		

**Table S3.**  $\pi\cdots\pi$  ring interaction and  $\pi\dots$ gold distances (Å) and angles ( $^{\circ}$ ) for compound **2**<sup>a</sup>

$\pi\cdots\pi$ ring interaction							
Cg(I)	Cg(J)	Symmetry Cg(j)	Cg(I)-Cg(J)	$\alpha$	$\beta$	$\gamma$	slippage
pyN4	pyN4	x, -1/2-y, -1/2+z	3.774(3)	1.3(3)	24.3	24.8	1.552
pyN4	pyN4	x, -1/2-y, 1/2+z	3.775(3)	1.3(3)	24.8	24.3	1.584
pyN4	pyN5	x, -1/2-y, 1/2+z	3.714(3)	3.0(3)	22.9	21.3	1.445
pyN5	pyN4	x, -1/2-y, -1/2+z	3.713(3)	3.0(3)	21.3	22.9	1.349
$\pi\dots$ Au interaction							
pyN3	Au	1-x, -x, -z	3.763		15.77		

**Table S4.**  $\pi\cdots\pi$  ring interaction and  $\pi\dots$ gold distances (Å) and angles ( $^{\circ}$ ) for compound **3**<sup>a</sup>

$\pi\cdots\pi$ ring interaction							
Cg(I)	Cg(J)	Symmetry Cg(j)	Cg(I)-Cg(J)	$\alpha$	$\beta$	$\gamma$	slippage
pyN3	pyN5	-1-x, -y, -1-z	3.743(3)	2.9(3)	24.3	27.2	1.542
pyN5	pyN3	-1-x, -y, -1-z	3.743(3)	2.9(3)	27.2	24.3	1.708
pyN3	pyN5	-x, -y, -1-z	3.650(3)	2.9(3)	22.1	20.1	1.375
pyN5	pyN3	-x, -y, -1-z	3.651(3)	-2.9(3)	20.1	22.1	1.253
$\pi\dots$ Ag interaction							
pyN4	Ag1		3.557		16.75		
pyN4	Ag1		3.392		14.73		

**Table S5**  $\pi\cdots\pi$  ring interaction and  $\pi\dots$ gold distances (Å) and angles ( $^{\circ}$ ) for compound **4**<sup>a</sup>

$\pi\cdots\pi$ ring interaction							
Cg(I)	Cg(J)	Symmetry Cg(j)	Cg(I)-Cg(J)	$\alpha$	$\beta$	$\gamma$	slippage
pyN11	pyN12	1-x, 1-y, -z	3.588(12)	4.	17.6	21.3	1.085
pyN12	pyN11	1-x, 1-y, -z	3.588(12)	4.	21.3	17.6	1.301
pyN12	pyN13	x, -1+y, -1+z	3.938(11)	9.	26.4	25.0	1.754
pyN13	pyN12	x, 1+y, 1+z	3.938(11)	9.	25.0	26.4	1.666
pyN10	pyN15	1+x, y, z	4.016(12)	10.	21.9	30.4	1.498
pyN15	pyN10	-1+x, y, z	4.015(12)	10.	30.4	21.9	2.033
$\pi\dots$ Metal interaction							

pyN10	Ag3	-	3.467		25.66		
pyN11	Ag2	1+x, y, z	3.558		21.67		
pyN13	Ag4	1-x, 3-y, 1-z	3.552		17.81		
pyN14	Ag3	1-x, 2-y, 1-z	3.450		15.18		
pyN15	Au1	-	3.608		9.44		

<sup>a</sup> Cg(I)-Cg(J): distance between ring centroids;  $\alpha$ : dihedral angle between planes Cg(I) and Cg(J);  $\beta$ : angle Cg(I)  $\rightarrow$  Cg(J) vector and normal to plane I;  $\gamma$ : angle Cg(I)  $\rightarrow$  Cg(J) vector and normal to plane J; slippage: distance between Cg(I) and perpendicular projection of Cg(J) on ring I.

## ESI mass spectrometry

The ESI mass spectrum of the  $[\text{Ag}(\text{pyNP})(\text{Au}(\text{CN})_2)_2]_2$  complex dissolved in acetonitrile is reported in Figure 10. The molecular ion is absent. However, several peaks that may be assigned to ion fragments or to condensation or ligand exchange pathways occurring either in solution or in the gas phase environment of the mass spectrometer are clearly detectable. All the following ion assignments are based on experimental mass distributions that nicely fit with the calculated isotopic distributions. Comparison among experimental and calculated mass distributions are reported for a couple of ions as examples in the following figures. The base peak of the spectrum is centered around  $m/z$  523 and is due to the  $(\text{pyNP})_2\text{Ag}^+$  fragment (Figure 11). The peak centered at  $m/z$  1058 corresponds to the ion  $\text{Ag}_4(\text{pyNP})(\text{NO}_3)_2(\text{EtOH})(\text{Au}(\text{CN})_2)_2^+$ . It may be considered as a fragment of the dimer of the original complex which underwent ligand exchange with an ethanol molecule. Traces of ethanol are present in the reaction environment since it was used as a solvent for the synthesis of the complex. Moreover, two dicyanoaurate ions were displaced by two nitrate ions, which are present in the reaction mixture since the complex was synthesized starting from silver nitrate. Unfortunately, no insights about ion structure can be drawn from MS/MS experiments, because these mass spectra were too noisy to allow sound interpretation; nevertheless, it may be safely assumed that both the  $\text{Au}(\text{CN})_2^-$  moieties were originally bridged between two Ag atoms before fragmentation occurred. The multiplet centered at  $m/z$  923 is assigned to  $\text{Ag}_4(\text{HCN})(\text{NO}_3)_2(\text{EtOH})_2(\text{Au}(\text{CN})_2)_2^+$ . Also this ion is a conceivable fragment of the dimer of the complex. Here, two pyNP ligands were replaced by two EtOH and one HCN molecules. This latter species likely arises from protonation of a cyanide moiety taking place in solution or, most probably, in the gas phase. Further fragmentation of the dimer complex, with complete loss of the ligands and of one silver atom, leads to the ion  $\text{Ag}_3(\text{H})(\text{NO}_3)(\text{Au}(\text{CN})_2)_2^+$ , corresponding to the peak at  $m/z$  886. In this case, protonation of the complex is assumed in order to fit with both the  $m/z$  ratio and the charge of the detected ion. The original monomer  $[\text{Ag}(\text{pyNP})(\text{Au}(\text{CN})_2)_2]$  complex undergoes extensive fragmentation and/or ligand exchange under the experimental conditions used here, as there is only one signal clearly assigned to it, falling at  $m/z$  656. This peak is assumed to correspond to the ion  $\text{Ag}_2(\text{HCN})(\text{CH}_3\text{CN})_4(\text{Au}(\text{CN})_2)^+$ . Here, ligand exchange with the acetonitrile solvent employed to record the spectra largely occurs. Moreover, protonation of the cyanide moiety is again observed, and the formed hydrogen cyanide likely acts as a ligand for silver. Finally, the peak at  $m/z$  789 corresponds to the ion  $\text{Ag}_3(\text{NO}_3)(\text{bipy-H})(\text{Au}(\text{CN})_2)^+$  (Figure 12), where bipy-H stands for the bipyridyl radical. This species is an impurity present in the reaction environment, which displaces one pyNP ligand and behaves as a bidentate ligand which binds two Ag atoms.

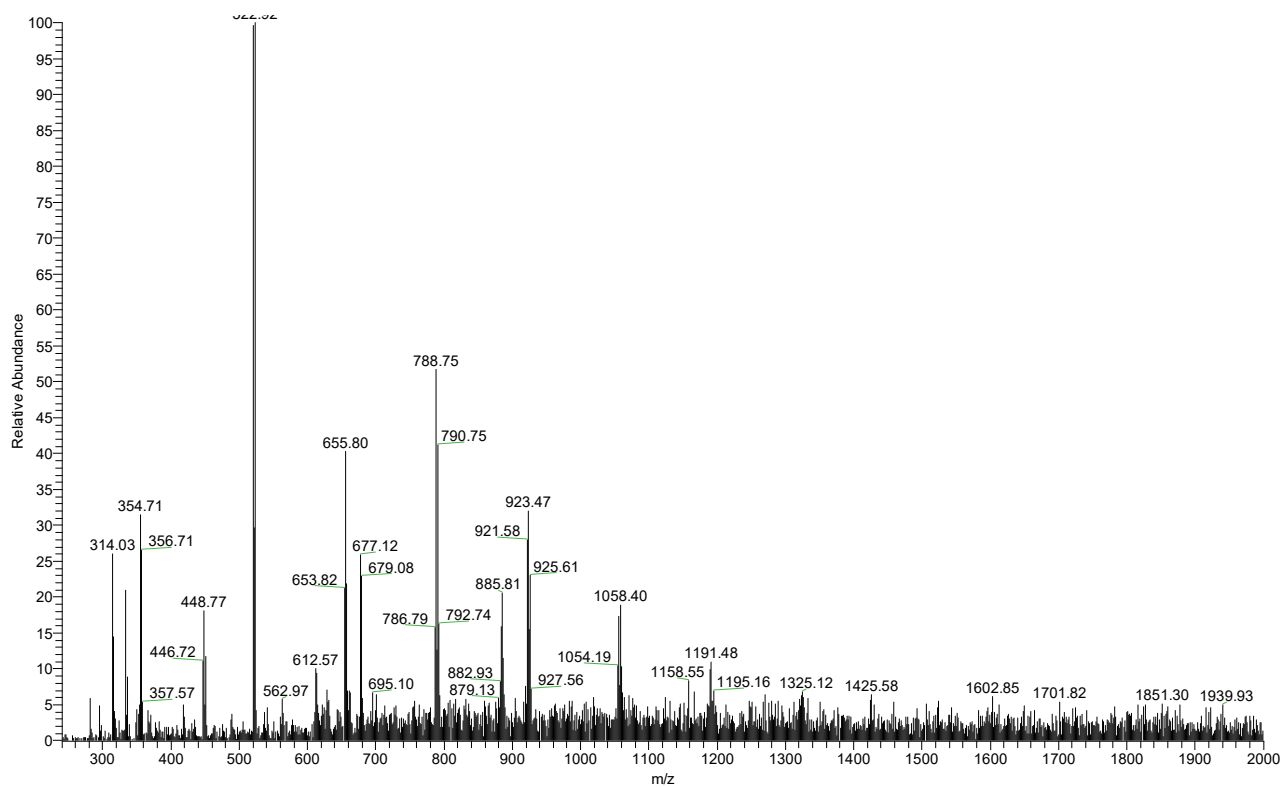


Figure S1. ESI-MS spectrum of the  $[\text{Ag}(\text{pyNP})(\text{Au}(\text{CN})_2)_2]$  complex.

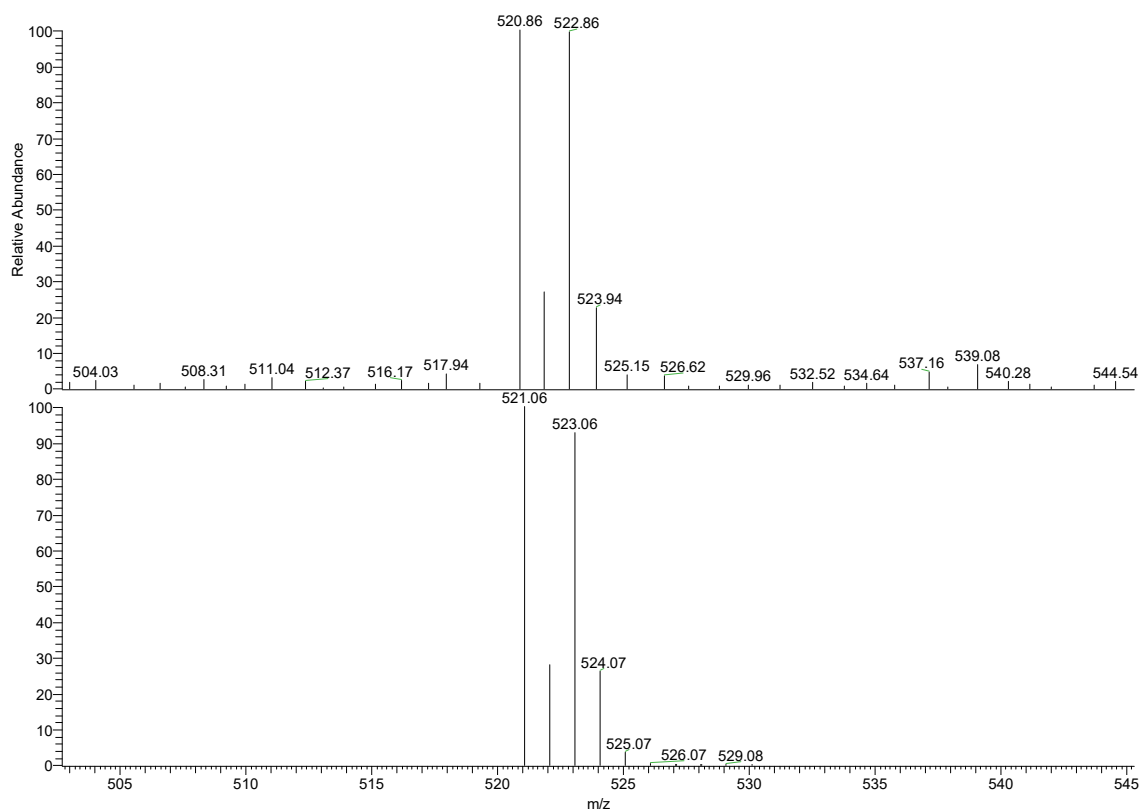


Figure S2. Comparison among experimental (above) and calculated (below) mass distributions for the  $(\text{pyNP})_2\text{Ag}^+$  ion.

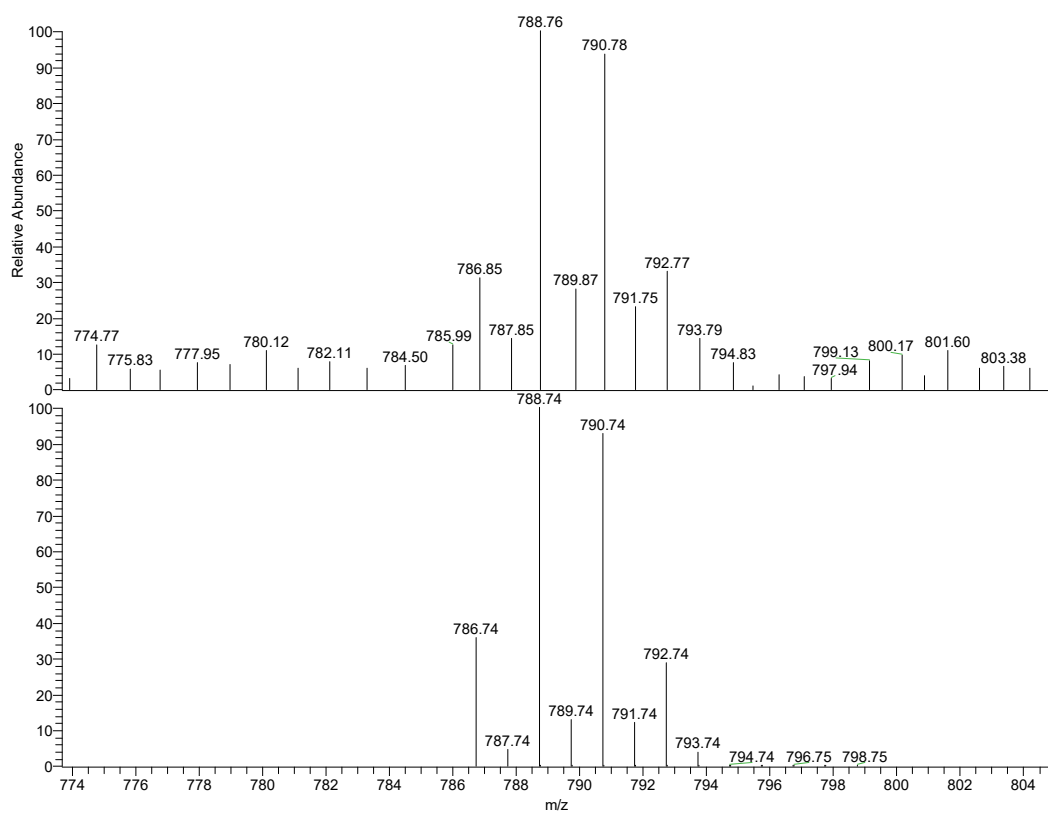


Figure S3. Comparison among experimental (above) and calculated (below) mass distributions for the  $\text{Ag}_3(\text{NO}_3)(\text{bipy-H})(\text{Au}(\text{CN})_2)^+$  ion.